PLOS | NEGLECTED TROPICAL DISEASES

RESEARCH ARTICLE

H^+ channels in embryonic *Biomphalaria glabrata* cell membranes: Putative roles in snail host-schistosome interactions

Brandon J. Wright[1‡], Utibe Bickham-Wright[2‡], Timothy P. Yoshino[2]*, Meyer B. Jackson[1]*

1 Department of Neuroscience, School of Medicine and Public Health, University of Wisconsin-Madison, Madison, Wisconsin, United States of America, **2** Department of Pathobiological Sciences, School of Veterinary Medicine, University of Wisconsin-Madison, Madison, Wisconsin, United States of America

‡ co-first authors
* mbjackso@wisc.edu (MBJ); yoshinot@vetmed.wisc.edu (TPY)

OPEN ACCESS

Citation: Wright BJ, Bickham-Wright U, Yoshino TP, Jackson MB (2017) H^+ channels in embryonic *Biomphalaria glabrata* cell membranes: Putative roles in snail host-schistosome interactions. PLoS Negl Trop Dis 11(3): e0005467. https://doi.org/10.1371/journal.pntd.0005467

Editor: Matty Knight, George Washington University School of Medicine and Health Sciences, UNITED STATES

Received: October 28, 2016

Accepted: March 7, 2017

Published: March 20, 2017

Data Availability Statement: Data are available from the NCBI database. The PredBgHVCN1-like accession number is XM_013231505, and the a-tubulin accession number is XP_013094834.1.

Funding: This work was supported by NIH/NIAID Grant No. R01AI015503 to TPY and B. glabrata snails and schistosome-infected mice were provided by the NIAID Schistosomiasis Resource Center at the Biomedical Research Institute (Rockville, MD) through NIH-NIAID Contract

Abstract

The human blood fluke *Schistosoma mansoni* causes intestinal schistosomiasis, a widespread neglected tropical disease. Infection of freshwater snails *Biomphalaria spp.* is an essential step in the transmission of *S. mansoni* to humans, although the physiological interactions between the parasite and its obligate snail host that determine success or failure are still poorly understood. In the present study, the *B. glabrata* embryonic (Bge) cell line, a widely used *in vitro* model for hemocyte-like activity, was used to investigate membrane properties, and assess the impact of larval transformation proteins (LTP) on identified ion channels. Whole-cell patch clamp recordings from Bge cells demonstrated that a Zn^{2+}-sensitive H^+ channel serves as the dominant plasma membrane conductance. Moreover, treatment of Bge cells with Zn^{2+} significantly inhibited an otherwise robust production of reactive oxygen species (ROS), thus implicating H^+ channels in the regulation of this immune function. A heat-sensitive component of LTP appears to target H^+ channels, enhancing Bge cell H^+ current over 2-fold. Both Bge cells and *B. glabrata* hemocytes express mRNA encoding a hydrogen voltage-gated channel 1 (HVCN1)-like protein, although its function in hemocytes remains to be determined. This study is the first to identify and characterize an H^+ channel in non-neuronal cells of freshwater molluscs. Importantly, the involvement of these channels in ROS production and their modulation by LTP suggest that these channels may function in immune defense responses against larval *S. mansoni*.

Author summary

Schistosoma mansoni is one of four major species of human blood flukes that, together, infect over 250 million people worldwide. Transmission of *S. mansoni* to humans requires infection of freshwater intermediate host snails, *Biomphalaria* spp., in order to complete its life cycle. The *B. glabrata* embryonic (Bge) cell line, derived from a Puerto Rican strain of snail host shares characteristics with circulating hemocytes, the molluscan immune cells, and serves as an *in vitro* model for snail immune function. Electrical recordings from Bge cells demonstrated the presence of H^+ channels that allow hydrogen ions (H^+)

HHSN272201000005I for distribution through BEI Resources. UBW was supported by a UW-Madison Advanced Opportunity Fellowship (SciMed Graduate Research Scholars Program) and NIH T32 training grant support from the Biotechnology Training Program (5T32GM08349) and Cellular and Molecular Parasitology Training Program (T32AI007414). The funders had no role in study design, data collection and analysis, decision to publish, or preparation of the manuscript.

Competing interests: The authors have declared that no competing interests exist.

to cross the membrane. Furthermore, blocking these channels inhibited the production of reactive oxygen species (ROS), an immune defense mechanism shared by Bge cells and hemocytes. Interestingly, Bge cell exposure to proteins produced by *S. mansoni* larvae exerted the opposite effect, enhancing H^+ movement across the cell membrane. An H^+ channel-encoding gene was expressed in both Bge cells and hemocytes suggesting that hemocytes may share similar functions with Bge cells.

Introduction

Schistosomiasis, a neglected tropical disease afflicting over 250 million people worldwide [1], is caused by parasitic flatworms of the genus *Schistosoma*. *Schistosoma* spp. have a two-host life cycle involving sexual reproduction within a mammalian host and asexual reproduction within a snail intermediate host. The pathology associated with the intestinal form of human schistosomiasis arises in chronic infections when eggs released by female worms occupying mesenteric veins become trapped in the liver (and other organs) and elicit an intense inflammatory response leading to the formation of granulomas that damage tissues and block circulation [2, 3]. Eggs from ruptured intestinal capillaries exit the host by fecal excretion, and upon exposure to freshwater, hatch to release the free-swimming snail-infective miracidia. Upon infection of snails, miracidia transform through two sporocyst stages, ultimately completing their life cycle by the production and release of free-swimming cercariae, the human-infective stage [4]. Because of the absolute dependency of human schistosome transmission on the snail host, one of the keys to sustained control of schistosomiasis is to block or eliminate the snail's participation in the life cycle.

The freshwater snail *Biomphalaria glabrata* serves as the most common invertebrate host of *S. mansoni*, the most widely distributed species of *Schistosoma* [5]. Hemocytes (phagocytic immune cells) of *B. glabrata*, genetically-selected for susceptibility or resistance to infection by larval *S. mansoni*, have been shown to react differentially to invading miracidia. Circulating hemocytes of susceptible strains do not recognize and kill invading larvae, whereas in resistant snails developing larvae are rapidly encapsulated by hemocytes and killed within 24–48 hours of infection [6–8]. Hemocyte larvicidal activity has been linked to the production and release of reactive oxygen species (ROS), mainly hydrogen peroxide (H_2O_2), and the reactive nitrogen species, nitric oxide [9, 10]. Although hemocytes of both resistant and susceptible *B. glabrata* strains produce H_2O_2, resistant hemocytes generate and release higher levels than susceptible cells [11], and this production appears to depend on the extracellular signal regulated protein kinase (Erk) [12]. However, a critical question arising from these observations is what are the signaling mechanisms that regulate ROS responses?

A critical period of larval development in the snail host is 24–48 hours post-infection, when the newly invading miracidium completes its transformation to the primary sporocyst stage. Larval killing depends on the ability of circulating hemocytes to recognize and encapsulate the newly formed sporocyst [4, 13–15]. Among various sporocyst factors that may be contributing to hemocyte reactivity are glycoproteins that are released during the miracidium-to-sporocyst transition. *In vitro* studies have shown that these larval transformation proteins (LTPs) [16] modulate phagocytic activity, motility, and ROS production in *B. glabrata* hemocytes [17–21], and disrupt hemocyte immune signaling [22–24]. However, questions regarding specific mechanisms by which LTPs modulate hemocyte immune responses remain unanswered.

For over four decades a cell line derived from embryos of a schistosome-susceptible strain of *B. glabrata*, the *B. glabrata* embryonic (Bge) cell line [25], has served as an *in vitro* model for

the study of larval schistosome-snail host interactions in schistosomiasis. Bge cells share many characteristics with *B. glabrata* hemocytes including their morphology, adhesive properties, phagocytic activity, and larval encapsulation response [26]. In fact, co-culture of Bge cells with *S. mansoni* larvae results in the development of the parasite from the miracidium to the final cercarial stage, similar to the development that occurs with susceptible *B. glabrata* strains [27–30]. We have therefore adopted Bge cells as an *in vitro* model system to study the molecular interactions between snail cells and *S. mansoni* LTP. Because ion channels in the plasma membrane of human immune cells, including eosinophils, macrophages, neutrophils and lymphocytes, play important roles in immune responses, often by regulating the production and release of ROS [31], we explored the role ion channels may play in signaling and ROS production in Bge cells. Using the whole cell patch clamp technique, we discovered an LTP-sensitive H^+ channel that serves as the dominant ion conductance of Bge cell membranes. In addition, using a fluorescent probe to measure intracellular ROS, we also found that this channel mediates the production of ROS, thus suggesting a possible function for H^+ channels in snail immune responses.

Materials and methods

All animal care and procedures were approved by the Institutional Animal Care and Use Committee of the University of Wisconsin-Madison under protocol V00640.

Maintenance of Bge cells

The Bge cell line was originally obtained from American Type Culture Collection (ATCC CRL 1494) and is currently available through the BEI Resources (https://www.beiresources.org). Cells were maintained at 26˚C under normoxic conditions in complete Bge (c-Bge) medium consisting of 22% Schneider's *Drosophila* Medium, 0.45% lactalbumin enzymatic hydrolysate, and 7.2 mM galactose supplemented with 10% heat-inactivated fetal bovine serum and 1% penicillin/streptomycin [25, 28]. Bge cells were passaged at 80% confluency.

Collection of larval transformation proteins (LTPs)

S. mansoni eggs were isolated, hatched, and miracidia cultured *in vitro* as previously described [28]. Approximately ~ 5000 miracidia/mL in Chernin's balanced salt solution (CBSS; 47.9 mM NaCl, 2.0 mM KCl, 0.5 mM Na_2HPO_4, 0.6 mM $NaHCO_3$ 1.8 mM $MgSO_4$, 3.6 mM $CaCl_2$ and pH 7.2) [32] supplemented with glucose (1 mg/mL), trehalose (1 mg/mL), penicillin G (100 units/mL) and streptomycin sulfate (0.05 mg/mL) adjusted to pH 7.2 (CBSS+) were then plated in a 24-well tissue culture plate and incubated at 26˚C under normal atmospheric conditions to allow *in vitro* transformation of miracidia to primary sporocysts. The LTP-containing culture medium was collected after 48 hr, and the newly transformed primary sporocysts were washed once with CBSS+. The LTP and CBSS+ wash were combined, filtered with a 0.45 μm Nalgene syringe filter (Thermo Scientific, Waltham, MA), and concentrated using 3 kDa molecular weight cut-off ultrafiltration tubes (Amicon Ultra Centricon, Billerica, MA). A NanoDrop ND-1000 spectrophotometer (NanoDrop Technologies, Wilmington, DE) was used to determine the protein concentration, after which a protease inhibitor cocktail (Calbiochem, Billerica, MA) was added. Multiple collections of LTP were pooled and stored in aliquots at -20˚C. To denature LTP, pools were boiled at 100˚C for 5 min.

Patch-clamp recording

Bge cells (~4 x 10^6) were plated in 60x15 mm petri dishes in c-Bge medium, and allowed to attach overnight. In order to make recordings under defined ionic conditions, cells were

washed 3X with CBSS before recording and kept in this buffer during subsequent manipulations. In experiments involving the treatment of Bge cells with $ZnCl_2$, 10 mM HEPES replaced NaH_2PO_4 in CBSS due to the insolubility of $Zn_3(PO_4)_2$. Adherent cells were viewed with an Axioskop microscope equipped with a 63X water-immersion objective (Carl Zeiss, Thornwood, NY). Bge cells were imaged with a CCD camera and viewed on a monitor. Patch electrodes fabricated from borosilicate glass capillaries had resistances of 3–7 MΩ when filled with a solution containing (in mM) 60 K-gluconate, 1 $CaCl_2$, 1 $MgCl_2$, 1 Mg-ATP, 10 HEPES, and 5 EGTA. The bathing solution for recordings was a slightly modified version of CBSS consisting of (in mM): 47 NaCl, 2 KCl, 0.5 NaH_2PO_4, 0.6 $NaHCO_3$, 1.8 $MgSO_4$, 3.6 $CaCl_2$. The pH of the pipette solution and external CBSS was adjusted to 5 or 7 with KOH or HCl. Modified versions of the internal and external solutions are stated in the Results section where they are used. Pressure-ejection pipettes were modified patch electrodes with tip diameters of ~2 μm. A Picospritzer II (General Valve Corp.) was used to apply 5–10 PSI of pressure to ejection pipettes.

Patch clamp recordings were made with an Axopatch 200B amplifier (Molecular Devices, Sunnyvale, CA), with data read into a PC through a Digidata 1440 A interface. The computer program pClamp 10 (Molecular Devices) controlled data acquisition, voltage steps, and pressure application by the Picospritzer. Data were filtered with a low-pass Bessel filter at 2 kHz before digitization at 10 kHz.

Reactive oxygen species (ROS) measurement

The fluorescent probe 2'7'-dichlorofluorescein-diacetate (DCFH-DA; Sigma-Aldrich, St. Louis, MO) was used to measure ROS production in Bge cells following a method described previously with hemocytes [33]. Bge cells (~1.5 x 10^5) in suspension were washed 3X with CBSS before incubation in CBSS (control), CBSS containing either 30 μg/mL LTP, 1 mM $ZnCl_2$ or 30 μg/mL LTP + 1 mM $ZnCl_2$ for 1 hr at 26˚C. After treatment, cells were washed 3X with CBSS and centrifuged at 1000 rpm for 10 min. The final cell pellets were then re-suspended in 150 μL of CBSS containing 10 μM DCFH-DA, and distributed in three wells of a 96-well black-walled plate (BD Falcon). The oxidation of DCFH-DA to fluorescent 2'7'-dichlorofluorescein (DCF) was measured in triplicate at 10 min intervals for up to 60 min using a Bio-Tek Synergy fluorescence plate reader (Winooski, VT) with excitation and emission wavelengths of 485 ± 20 and 528 ± 20, respectively. Data analysis was conducted with Origin software (Microcal, Northhampton, MA, USA). Five independent replicates of each experiment were conducted, with the raw data presented as mean ± SEM, and ratios of means of treated groups to controls presented separately.

Amplification and sequencing of H^+ channel transcripts

For molecular analysis of H^+ channels, the hydrogen voltage gated channel 1 (HVCN1) gene was identified in the nonredundant NCBI database, and sequence comparisons were conducted with PCR products from Bge cells and *B. glabrata* hemocytes. Schistosome-susceptible (NMRI) and resistant (BS-90) *B. glabrata* strains were maintained in laboratory colonies in 10-gallon aquaria at 26˚C under 12:12 hr light/dark cycling. Hemolymph, containing hemocytes, was collected by headfoot retraction [34] and immediately transferred to Eppendorf tubes containing an equal volume of CBSS on ice. Hemocytes were then pelleted by centrifugation at 1000 RPM for 10 min and washed 3 times in CBSS. Bge cells, grown in a flask to ~80% confluency, were detached mechanically using a cell scrapper, transferred to a 15 mL conical tube and pelleted by centrifugation as described for hemocytes.

Total RNA was extracted from Bge cells and hemocytes of both *B. glabrata* strains using TRIzol reagent. Normalized concentrations of isolated total RNA samples were subjected to

cDNA synthesis reactions using the GoScript™ Reverse Transcription System (Promega Corp., Madison, WI). The cDNA was then used as the template for PCR using primers for the *B. glabrata* voltage-gated H^+ channel 1-like gene (*Bg*HVCN1-like; Forward 5'-TGCTATG GGCTTAGCTTACTTC-3'; Reverse 5'-ATGTAGGGTCTTCAAACCATTCT-3') that were designed using the predicted mRNA sequence for the gene with the National Center for Biotechnology Information (NCBI) database (Accession number XM_013231505). The expected amplicon size is ~362 bp, ~65% of the coding DNA sequence. As a positive control, primers for *B. glabrata* α–tubulin (Forward 5' -GTGAGACTGGCTGTGGTAAA-3'; Reverse 5' -GGG AAGTGAATCCTGGGATATG-3') with Accession number XP_013094834.1 were used to amplify an expected product of ~643 bp. Gel electrophoresis of the PCR products was performed followed by Big Dye sequencing at the University of Wisconsin Biotechnology Center DNA Sequencing Facility (Madison, WI). The resulting nucleotide sequences were used in a search using BLASTn search against the non-redundant nucleotide NCBI database to confirm that the PCR amplified product encoded an HVCN1-like protein.

Analysis and statistics

Patch clamp data were analyzed with Clampfit (Molecular Devices, Sunnyvale, CA) and Origin Pro (Microcal, Northhampton, MA). One-way RM-ANOVA and post-hoc statistical analyses were conducted in Origin Pro to assess significance. Results are presented as means ± SEM. The asterisks (*) represent $p < 0.05$ in all figures.

Results

Whole cell patch clamp recordings were made from Bge cells to explore their membrane properties. Voltage steps from -75 to 25 mV for 500 msec induced an outward current that activated rapidly and then weakly inactivated in ~10–20 msec before stabilizing (Fig 1A, control trace, top). To identify the ions responsible for this current, we manipulated the composition of the recording solutions. When Cl^- was replaced by gluconate in the internal and bathing solutions, voltage steps induced currents similar to those seen with control solutions (Fig 1A, second trace from top). Further substitution of Cs^+ for K^+ in the internal solution reduced the current to roughly 68% of control currents (Fig 1A, third trace from top). The mean peak and plateau current amplitudes for these solutions are shown in Fig 1B. For gluconate and Cs^+ substitution, current amplitudes were not significantly different from the control. Thus, Cl^- and K^+ replacement experiments indicated that these are not major permeating ions. In addition, comparisons of the Nernst potentials (equilibrium potential for each ion based on internal and external concentrations) with reversal potentials in current-voltage relationships did not support channels selective for Na^+ or Ca^{2+} (Supplemental S1 Fig). These results suggested that the major ions in our recording solutions do not permeate the membranes of Bge cells.

H^+ channels play important roles in many types of immune cells [35], so we explored the possibility that H^+ channels reside in the membranes of Bge cells. Subjecting Bge cells to pH gradients (by adjusting the pH of the pipette and bathing solutions–see Methods) [36] altered the current elicited by voltage steps and shifted the relationship between current and voltage (Fig 2). A gradient of two pH units (pH 5_{in}/pH 7_{out}) reduced the current amplitude at all voltages and shifted the reversal potential in the plot of peak current versus voltage in the negative direction by 17.5 mV (Fig 2B, dashed line). Reversing the pH gradient (pH 5_{out}/pH 7_{in}) shifted the peak current-voltage plot in the opposite direction with a positive shift in the reversal potential of 27.5 mV (Fig 2B, dotted line). Plots of plateau current versus voltage showed similar shifts (Supplemental S2 Fig). Table 1 presents the reversal potentials along with the Nernst potentials for H^+. The shifts are in the direction of the H^+ Nernst potential but smaller in

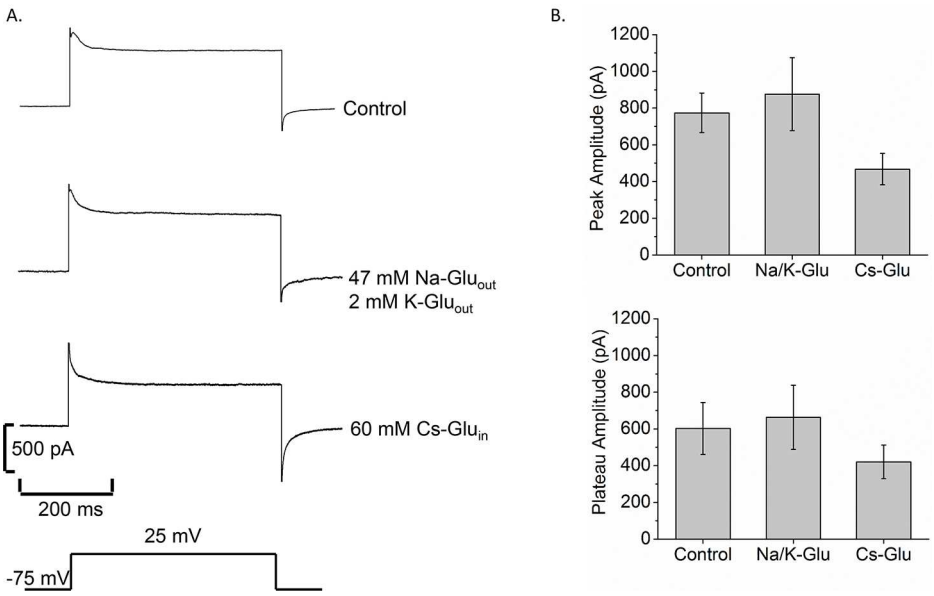

Fig 1. Bge cell membrane current is not carried by K^+ or Cl^-. A. Current traces in response to a voltage step from -75 mV to 25 mV for 500 msec for control solutions (top), 47 mM Na-Glu$_{out}$/2 mM K-Glu$_{out}$, with gluconate replacing Cl^- in the bathing solutions (second trace), and 60 mM Cs-Glu$_{in}$ replacing KCl in the internal solution (third trace). The bottom pulse represents the voltage applied to the cell. B. Bar graphs show the mean peak current (top), and mean plateau current (bottom) for each group. N = 15 (control); N = 7 (Na/K Glu); N = 5 (Cs-Glu).

https://doi.org/10.1371/journal.pntd.0005467.g001

magnitude because the H^+ concentration is much lower relative to the concentrations of other ions in the solutions. Channels permeable to other ions generally result in H^+ current reversal potential shifts that are less than the change in the H^+ Nernst potential [37]. The effects of pH

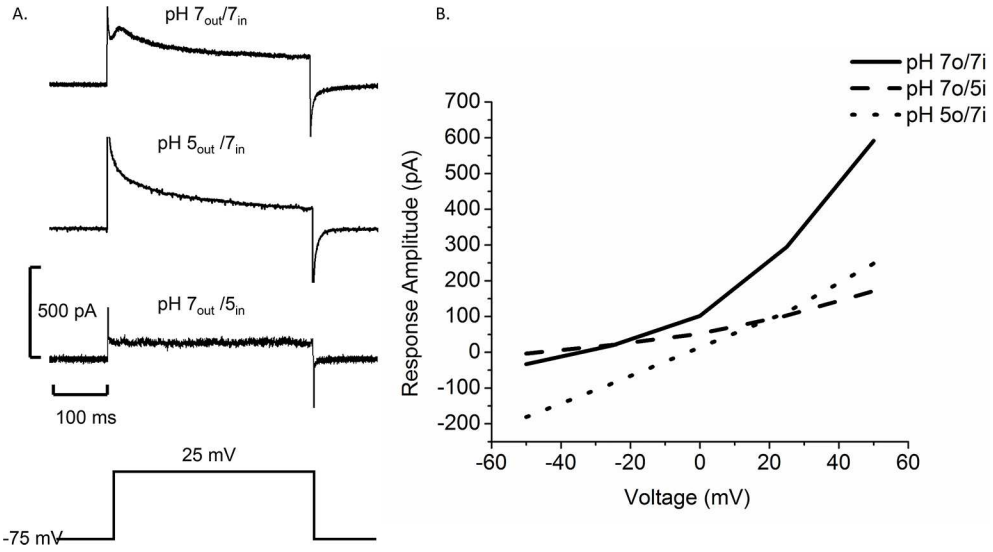

Fig 2. The pH gradient influences the voltage dependence of membrane current in Bge cells. A. Current traces show a control current with pH 7$_{out}$/pH 7$_{in}$ (top), pH 5$_{out}$/pH 7$_{in}$ (middle) and pH 7$_{out}$/pH 5$_{in}$ (bottom) (pulse from -75 mV to 25 mV indicated below). B. Plot of peak current versus voltage for steps varying from -50 mV to 50 mV. The solid curve represents control current in symmetrical pH (N = 4), the dotted curve represents pH 5$_{out}$/pH 7$_{in}$ (N = 5), and the dashed curve represents pH 7$_{out}$ /pH 5$_{in}$ (N = 5).

https://doi.org/10.1371/journal.pntd.0005467.g002

Table 1. pH-dependence of reversal potentials in Bge cells.

	$pH\ 7_{in}/pH\ 7_{out}$	$pH\ 5_{in}/pH\ 7_{out}$	$pH\ 7_{in}/pH\ 5_{out}$
V_{rev} (mV)	-32.5±2.53 (n = 4)	-50.0±0.65 (n = 5)	-5±1.5 (n = 5)
E_{H+} (mV)	0	-116	116

Table 1. The mean voltages at which the current reverses are shown in the top row. The computed equilibrium potential for H^+ (E_{H+}) is shown in the second row.

https://doi.org/10.1371/journal.pntd.0005467.t001

gradients on membrane currents are consistent with the presence of an H^+ channel in Bge cell membranes.

As an additional test for the presence of H^+ channels we applied the H^+ channel blocker Zn^{2+} [36, 38]. Pressure application of 1 mM $ZnCl_2$ from a glass pipette onto a Bge cell significantly reduced both peak and plateau currents elicited by voltage steps from -50 to 20 mV (Fig 3A). This blockade was reversible, as demonstrated by current recovery after $ZnCl_2$ removal (Fig 3A, wash trace). Time course plots in which $ZnCl_2$ was perfused onto cells through the bathing medium showed a 3.5-fold reduction in current amplitude (Fig 3B and 3C), from 621 ± 4 pA to 177 ± 1 pA (N = 4), supporting the presence of H^+ channels in Bge cell membranes. Although other actions of Zn^{2+} cannot be ruled out, the block of membrane current is consistent with the presence of H^+ channels in Bge cells.

As larval schistosome proteins have been shown to modulate a variety of snail hemocyte immune functions [14, 15], we tested the effects of *S. mansoni* LTP on Bge cell membrane current. Pressure application of LTP onto Bge cells dramatically increased the peak and plateau currents evoked by steps from -50 mV to 20 mV (Fig 4A). LTP increased the current significantly by over 2-fold (478 ± 6 pA) compared to control (212 ± 4 pA), and this increase only partially reversed with a 17% decrease (397 ± 7 pA) following removal of LTP. Recovery was slow, and 5 min after LTP removal the current had decreased only slightly (Fig 4B and 4C).

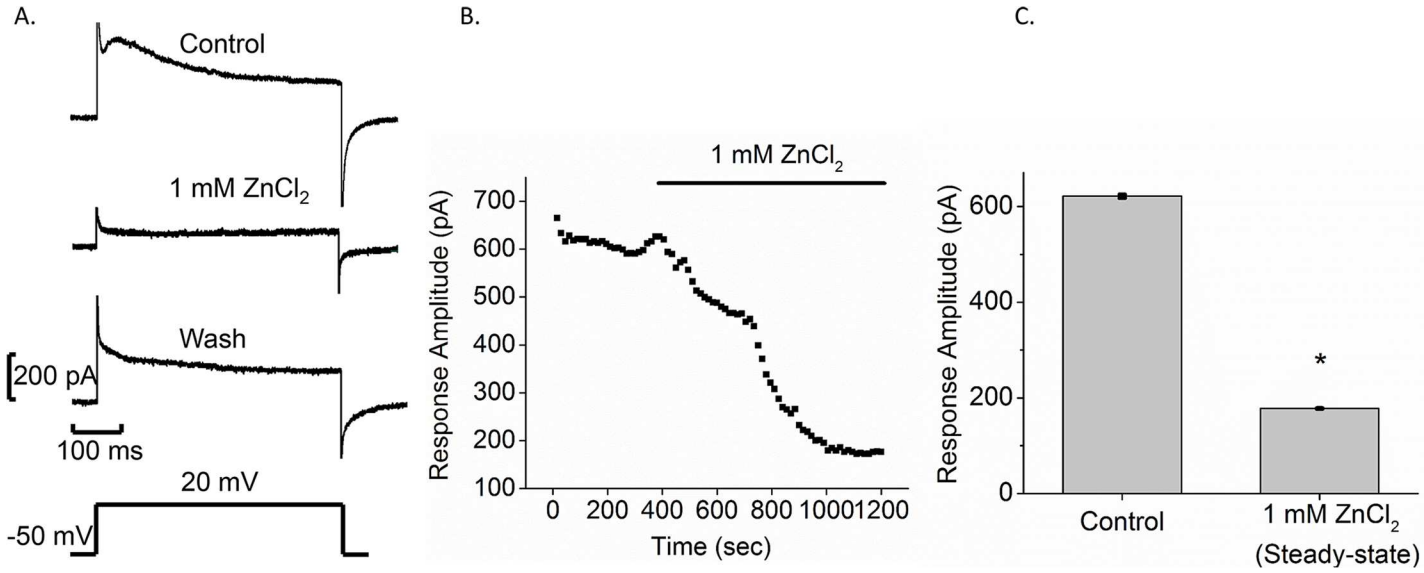

Fig 3. $ZnCl_2$ blocks membrane current in Bge cells. A. Control response to a voltage step (from -50 mV to 20 mV indicated below) (top). One mM $ZnCl_2$ was pressure applied onto Bge cells (middle). Wash response was measured10 min after post-$ZnCl_2$ removal (lower). B. Time course plot is presented for perfusion of 1 mM $ZnCl_2$. The bar labeled 1 mM $ZnCl_2$ above represents the time of $ZnCl_2$ application. C. Bar graphs show the mean current amplitude for control and in the presence of 1 mM $ZnCl_2$ after full effect was reached (mean ± SEM; N = 4; *p < 0.05).

https://doi.org/10.1371/journal.pntd.0005467.g003

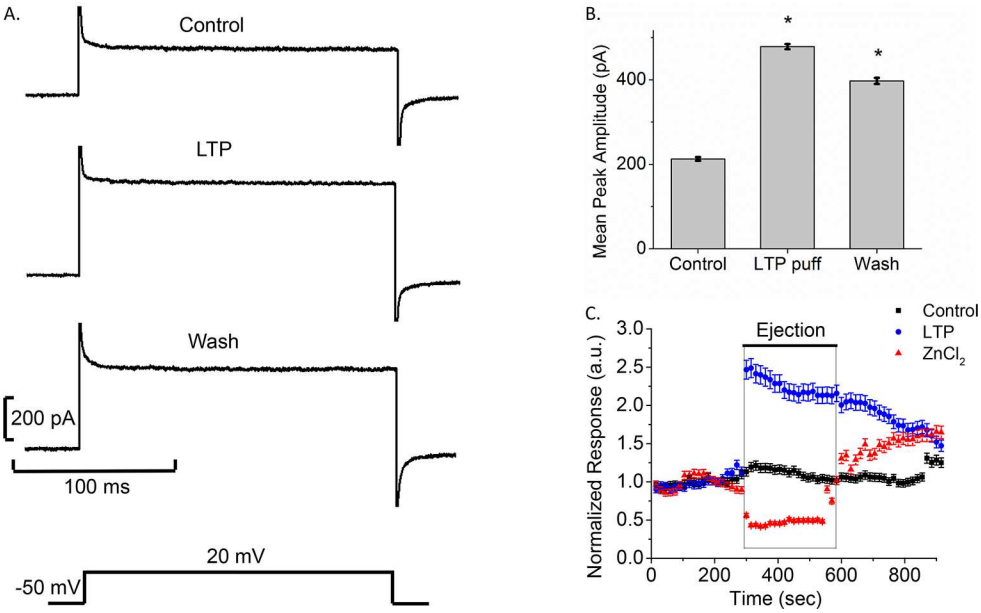

Fig 4. Larval transformation proteins (LTP) increase current amplitude in Bge cells. A. Traces for control (pre-LTP), during LTP pressure application (LTP), and washout (pulses from -50 mV to 20 mV as indicated below). B. Bar graphs show the mean peak amplitudes for each case (mean ± SEM; N = 5; *p < 0.05). C. LTP and $ZnCl_2$ have opposite effects. Normalized time course is shown for control (black), $ZnCl_2$ (red), and LTP (blue). The black bar above (labeled ejection) represents time of pressure application. Baseline responses were collected for 5 min, and the test solution applied for 5 min. For the control experiments, cells were puffed with CBSS. Responses were normalized by dividing by the average pre-puff baseline value. Note that puffing produces a more rapid effect than perfusion (compare with Fig 3). (mean ± SEM; N = 4-Control, 4-$ZnCl_2$, 5-LTP).

https://doi.org/10.1371/journal.pntd.0005467.g004

Plotting current versus time also illustrated the opposite effects of LTP and $ZnCl_2$ on Bge cells (Fig 4C). This plot showed a >2-fold increase in current amplitude in the presence of LTP (Fig 4C blue circles) and a >2-fold reduction in the presence of $ZnCl_2$ (Fig 4C, red triangles) compared to control (Fig 4C black squares). The reversal of block by $ZnCl_2$ was rapid and essentially complete, while the reversal of enhancement by LTP was slow. Moreover, when heat-denatured LTP was pressure-applied onto Bge cells, we observed no significant change compared to control current amplitudes (Fig 5C and 5D), indicating that the action of LTP on H^+ channels depends on heat-labile factors.

To determine whether LTP increased Bge cell membrane current by opening H^+ channels, we applied LTP and $ZnCl_2$ simultaneously, and observed no statistically significant change (Fig 5), indicating that $ZnCl_2$ counters the effect of LTP. Finally, we noted that current-voltage curves shifted in the presence of LTP and $ZnCl_2$; LTP caused a 9 mV right-shift from control, toward the H^+ Nernst potential, while $ZnCl_2$ caused a 23 mV left-shift, away from the H^+ Nernst potential (Fig 6). These results are consistent with the blockade of H^+ channels by $ZnCl_2$ and enhancement of H^+ channels by LTP.

Because H^+ channels contribute to ROS production in mammalian immune cells [35, 39], we measured the generation of ROS in Bge cells with the fluorescent probe 2'7'-dichlorofluorescein-diacetate (DCFH-DA). We observed a rapid and robust fluorescence increase that reflects constitutive ROS production. $ZnCl_2$ and LTP + $ZnCl_2$ inhibited this activity by ~50% compared to the untreated control ($F_{3,\ 16} = 24.26$, $p < 0.05$). These results demonstrate a linkage between H^+ channels and the production of ROS in Bge cells. LTP alone produced a small apparent increase in ROS production, but this increase was not statistically significant. This

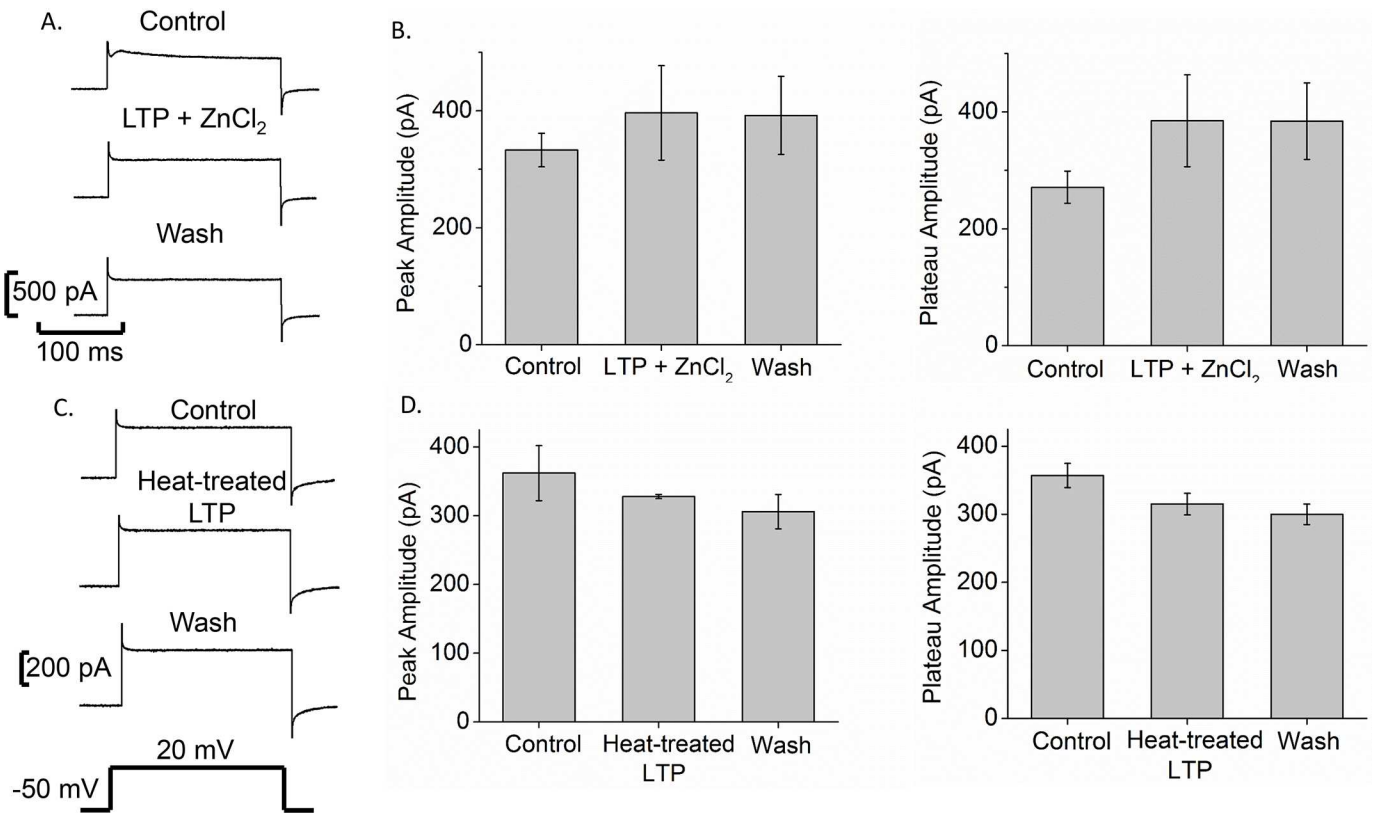

Fig 5. $ZnCl_2$ counters the effect of LTP on H^+ current in Bge cells. A. Simultaneous $ZnCl_2$+LTP did not change peak current amplitude from control, although there was an ~100 pA difference in sustained current at the end of the pulse (from -50 mV to 20 mV indicated below). B. Bars show the mean peak and plateau current for each case (mean ± SEM, N = 10). C. Current traces from control (pre-puff), during heat-treated LTP (puff) and after washout show that heat-treated LTP does not significantly alter response amplitudes. D. Bar charts show mean peak and plateau current amplitudes before, during, and after application of heat-treated LTP (mean ± SEM, N = 3).

https://doi.org/10.1371/journal.pntd.0005467.g005

suggests that at control level of H^+ current in Bge cells, other factors limit ROS production (Fig 7A and 7B).

To identify putative H^+ channel proteins expressed by Bge cells and *B. glabrata* hemocytes we searched the *B. glabrata* genome (https://www.vectorbase.org/organisms/biomphalaria-glabrata) using Blastp for homologues of human HVCN1 protein. The closest match was an HVCN1-like protein (*Bg*HVCN1-like, Accession number. XM_013231505) with 31% identity to human HVCN1. This sequence contained the motif RLWRVTR, which is consistent with the H^+ channel consensus sequence RxWRxxR [36]. A segment of the predicted sequence was then used to design primers for polymerase chain reactions (PCR). Using cDNA from Bge cells and *B. glabrata* hemocytes (NMRI and BS-90 strains) as templates, PCR using the primers stated in the Methods section yielded amplicons of similar size with 99% sequence identity (E = 0.0) to the predicted *B. glabrata* HVCN1-like sequence (Supplemental S3 Fig). The amplified products encode 120 amino acid stretch of the 186 residues predicted for molluscan HVCN1-like protein. These results indicate that mRNA with the predicted sequence for a *Bg*HVCN1-like gene is present in both Bge cells and hemocytes.

Discussion

This investigation revealed the presence of functional ion channels in Bge cell membranes. pH manipulations altered the voltage dependence of membrane currents in a manner consistent

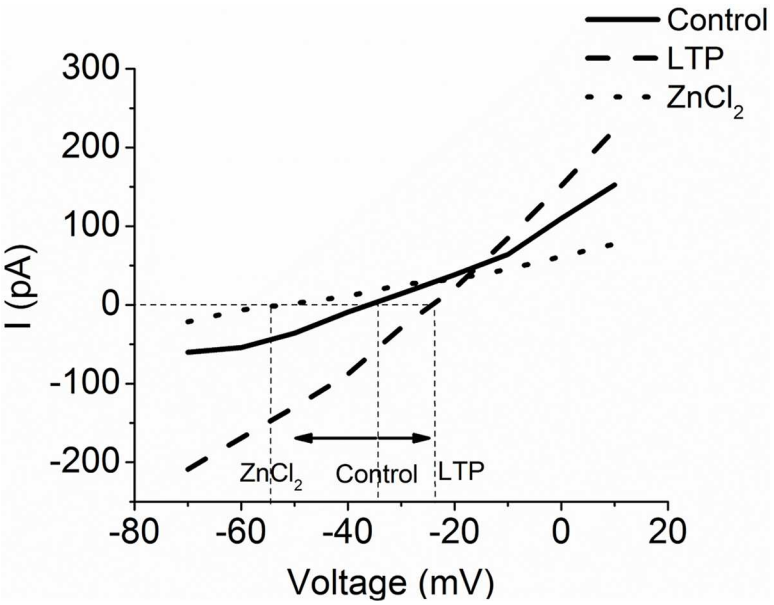

Fig 6. $ZnCl_2$ (dotted line) caused a left-shift of the current-voltage plot from control (solid line), while LTP (dashed line) caused a right-shift. This supports blockage and opening of H^+ channels, respectively. N = 4-Control, 6-$ZnCl_2$, 5-LTP.

https://doi.org/10.1371/journal.pntd.0005467.g006

with a dominant H^+ permeability. Since the H^+ concentration was several orders of magnitude lower than the other ions in our solutions, even low permeabilities to other ions can make large contributions to the observed reversal potentials and move them away from the H^+ Nernst potential. Thus, although currents did not reverse at the H^+ Nernst potential, the shifts were in the appropriate direction and supported the hypothesis that H^+ channels are the predominant ion permeability in the plasma membrane of Bge cells. We also found that the H^+

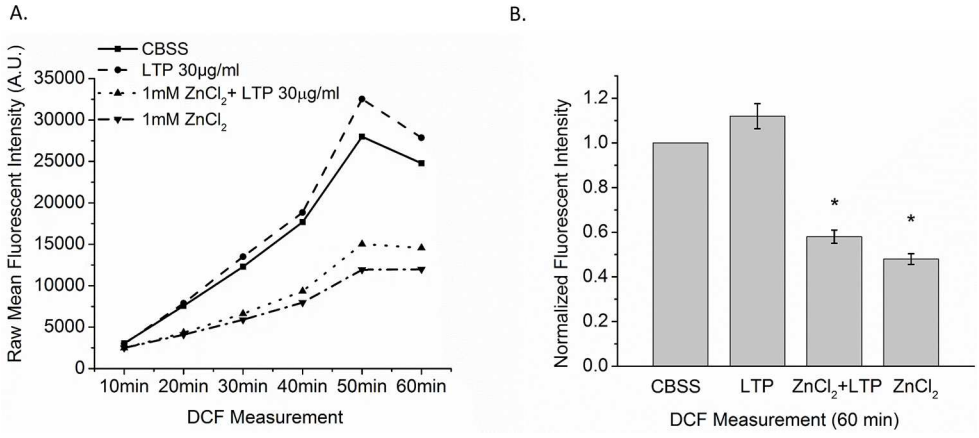

Fig 7. ROS production in Bge cells measured with DCFH-DA. Bge cells were exposed for 1 hr to CBSS only, LTP only, 1 mM $ZnCl_2$ only or LTP + 1 mM $ZnCl_2$. A. Raw DCFH-DA fluorescence was measured at 10 min intervals for 60 min and mean values plotted. $ZnCl_2$ (downward triangle with dashed-dotted line) and LTP + $ZnCl_2$ (upward triangle with dotted line) reduced fluorescence compared to CBSS control (square with solid line). LTP (circle with dashed line) had a weak, insignificant stimulatory effect. B. Bars show mean fluorescence with treatment normalized to constitutive control (CBSS) at 60 min. Bars represent means ± SEM. N = 5.

https://doi.org/10.1371/journal.pntd.0005467.g007

channel blocker Zn^{2+} significantly reduced the current through Bge cell membranes, providing additional support for the presence of H^+ channels. Finally, we identified and sequenced an HVCN1-like transcript expressed in both this snail cell line and *B. glabrata* hemocytes, suggesting a functional linkage between these cell types. Thus, three independent lines of evidence support the conclusion that Bge cells express functional H^+ channels. With few exceptions [40], previous studies focusing on ion channels in molluscs almost exclusively have involved neuronal cell systems and/or emphasized Na^+, K^+, Ca^{2+} or Cl^- channel activities [41–43]. To our knowledge, this is the first report of a functional H^+ channel in non-neuronal cells of freshwater gastropods.

Similar to the well documented association between H^+ channels and ROS production in mammalian immunocytes [39], we also found that blockade of the H^+ channel with Zn^{2+} significantly abrogated Bge cell ROS production, indicating a functional association between channel-mediated H^+ flux across the membrane and the oxidative response. This finding is significant since the formation and release of several ROS, especially H_2O_2, and RNS are known to be involved in the killing of larval *S. mansoni* by *B. glabrata* hemocytes [9, 10]. It is possible that, as in mammalian immune cells [39, 44], changes in membrane potential associated with ROS production also require a compensatory activation of H^+ channels to maintain pH balance in immunocyte-like molluscan cells. It is important to note that hemocytes from both resistant and susceptible strains of *B. glabrata* snails are capable of generating ROS [11, 32], but differ both qualitatively and quantitatively in their responses [11]. Since Bge cells were originally derived from a *S. mansoni*-susceptible Puerto Rican strain of *B. glabrata* [25], it is likely that hemocytes from a related susceptible strain (NMRI) also share both molecular and functional similarities to Bge cells. These shared characteristic have been well-documented in previous studies [26, 45, 46], supporting the use of this cell line as a hemocyte-like model, as well as a general model for *Biomphalaria*-schistosome interactions [29, 47]. Based on the presence and expression of the HVCN1-like gene in *B. glabrata* hemocytes, it is quite possible that voltage-gated H^+ channels are also involved in regulating cellular ROS production as demonstrated in Bge cells.

Proteins released during the *S. mansoni* miracidium-to-sporocyst transformation (LTP) have been shown to modulate a variety of functions in both hemocytes and Bge cells [14, 24, 45]. Such a role is supported by our finding of an LTP-induced potentiation of H^+ channel activity. Exposure to LTP elicited a rapid and sustained enhancement of Bge cell membrane current. Because the reversal potential moved toward the H^+ Nernst potential, it is likely that LTP increased the current through H^+ channels. This activity was heat-labile, suggesting that the channel-active LTP component(s) may be a protein(s) with irreversible or slowly reversing action. However, it remains unclear whether the regulation of Bge cell H^+ channels by schistosome LTPs results from factors thought to play a role in host-parasite compatibility [48–50] or other, yet unidentified, larval factors. The H^+ channel may play a role in co-evolutionary mechanisms, known to affect oxidant-antioxidant levels during parasite-host interaction [51]. Identifying the active components of LTP and determining whether this response reflects the action of a single or multiple species will require further investigation.

Despite the channel stimulating action of LTP, LTP treatment of Bge cells resulted in no statistically significant increase in ROS production. These results are consistent with previous findings that exposure of *B. glabrata* hemocytes to excretory-secretory products of larval *S. mansoni* exerted little effect on the production of ROS [52]. However, the question remains as to why LTP-stimulated H^+ channel activation failed to enhance ROS production. Based on the H^+ current data, it might be speculated that LTP binding to Bge cells is linked to the opening of H^+ channels through receptor-mediated activation of a channel-associated signaling pathway, possibly through interactions with pathogen recognition receptors such as fibrinogen-

related proteins, Toll-like receptors, or bacterial binding proteins that have been implicated in *B. glabrata* immunity [50, 53–55]. Mitogen-activated and extracellular-signal regulated protein kinases shown to function in molluscan immunity [12, 22] could also play a role in signaling to the H^+ channel. A final possibility is that LTP may be acting directly on the channel protein itself to induce opening. The consequence of H^+ channel modulation would be an alteration or disruption of H^+ ion balance and intracellular pH, but without stimulating ROS production. This may, in turn, serve as a potent anti-immune mechanism used by sporocysts for countering host ROS-mediated effector responses. Thus, H^+ channels, while serving an important role in maintaining pH balance within Bge cells and hemocytes, may also be manipulated by schistosome larvae to reduce their immune efficacy. Since Bge cells were originally derived from a *S. mansoni*-susceptible PR albino strain of *B. glabrata* [25], it is likely that hemocytes from a related susceptible strain (NMRI) also share sensitivity to H^+ channel–reactive anti-immune proteins, thereby supporting a compatible snail-schistosome interaction.

In conclusion, Bge cells possess a functional H^+ channel that is responsible for a dominant conductance of their plasma membrane. ROS production is dependent on H^+ channels. Exposure of cells to heat-labile LTP stimulates channel opening and H^+ flux, but has little if any effect on the generation of ROS. Although H^+ channels have not been tested directly in *B. glabrata* hemocytes, PCR amplification and amplicon sequencing demonstrated the presence of HVCN1-like transcripts in both susceptible and resistant *B. glabrata* strains. Thus, the association of the Bge cell H^+ channel activity with cellular ROS production and the channel's response to schistosome LTP suggest a role in regulating larval schistosome-snail interactions. Future identification of the specific mechanism(s) tying together these activities should provide important insights into host-parasite compatibility in this system.

Supporting information

S1 Fig. Current-voltage plots with control solutions and K-gluconate solutions used in Fig 1. Current was measured for voltage steps varying from -50 mV to 50 mV. E_{Ca} was computed as +120 mV based on a free [Ca^{2+}] of 200 nM computed from the EGTA and total [Ca^{2+}] of the pipette solution. E_{Na} has a large positive value that could not be determined because the pipette solution had no added Na^+. More positive voltage steps move the membrane toward the Nernst potentials for Na^+ and Ca^{2+}. The observed increases over the entire range with more positive voltage is not consistent with channels selective for Na^+ or Ca^{2+}.
(PDF)

S2 Fig. The pH gradient influences the voltage dependence of membrane current in Bge cells. Current-voltage plot for voltage steps varying from -50 mV to 50 mV. Fig 2 plotted peak current and this figure plots plateau current in symmetrical pH (solid curve, N = 4), pH 5-out/7-in (dotted curve, N = 6), and pH 7-out/5-in (dashed curve, N = 5).
(PDF)

S3 Fig. Gene sequence of HVCN1-like mRNA in Bge cells and *B. glabrata* hemocytes. PCR of cDNA derived from Bge cells and *B. glabrata* hemocytes of susceptible (NMRI) and resistant (BS90) snail strains revealed amplicons of predicted size (~362 bp) for *B. glabrata* HVCN1-like gene and the alpha tubulin (~643 bp) loading control (top). Multiple sequence alignment of HVCN1-like transcripts from Bge cells and hemocytes of *B. glabrata* (NMRI and BS90 strains) with the predicted sequence of *B. glabrata* HVCN1-like (PredBgHVCN1-like, Accession number XM_013231505) (bottom). The shaded regions show the minor differences in base pairs among the sequences.
(PDF)

Acknowledgments

We would like to thank Nathalie Dinguirard and Megan Mezera (Yoshino Lab) for animal care and hemocyte collection, and Chung-Wei Chiang (Jackson Lab) for his advice and helpful insights.

Accession numbers

Data are available from the NCBI database. The PredBgHVCN1-like accession number is XM_013231505, and the a-tubulin accession number is XP_013094834.1.

Author Contributions

Conceptualization: BJW UBW.

Data curation: BJW UBW.

Formal analysis: BJW UBW TPY MBJ.

Funding acquisition: TPY MBJ.

Investigation: BJW UBW.

Methodology: BJW UBW TPY MBJ.

Project administration: BJW UBW TPY MBJ.

Resources: UBW TPY.

Supervision: TPY MBJ.

Validation: BJW UBW TPY MBJ.

Visualization: BJW UBW.

Writing – original draft: BJW UBW TPY MBJ.

Writing – review & editing: BJW UBW TPY MBJ.

References

1. W.H.O. Schistosomiasis: number of people treated worldwide in 2016. Weekly epidemiological record 2015; 91(5):53–60.
2. Colley DG, Bustinduy AL, Secor WE, King CH. Human schistosomiasis. Lancet. 2014 (a); 383 (9936):2253–64. https://doi.org/10.1016/S0140-6736(13)61949-2 PMID: 24698483
3. Colley DG, Secor WE. Immunology of human schistosomiasis. Parasite Immunol 2014 (b); 36(8):347–57. https://doi.org/10.1111/pim.12087 PMID: 25142505
4. Yoshino TP, Gourbal B, Theron A. *Schistosoma* sporocysts. In: Jamieson B, editor. *Schistosoma*: Biology, Pathology and Control. Boca Raton, FL: Taylor Francis/CRC Press; 2017. p. 118–148.
5. Morgan JA, Dejong RJ, Adeoye GO, Ansa ED, Barbosa CS, Bremond P, et al. Origin and diversification of the human parasite *Schistosoma mansoni*. Mol Ecol 2005; 14(12):3889–902. https://doi.org/10.1111/j.1365-294X.2005.02709.x PMID: 16202103
6. Pan CT. Generalized and Focal Tissue Responses in the Snail, *Australorbis glabratus*, Infected with *Schistosoma mansoni*. Ann N Y Acad Sci. 1963; 113:475–85. PMID: 14088711
7. Sullivan JT, Richards CS. *Schistosoma mansoni*, NIH-SM-PR-2 strain, in susceptible and nonsusceptible stocks of *Biomphalaria glabrat*a: comparative histology. J Parasitol. 1981; 67(5):702–8. PMID: 7299581
8. Loker ES, Bayne CJ, Buckley PM, Kruse KT. Ultrastructure of encapsulation of *Schistosoma mansoni* mother sporocysts by hemocytes of juveniles of the 10-R2 strain of *Biomphalaria glabrata*. J Parasitol. 1982; 68(1):84–94. PMID: 7077450

9. Hahn UK, Bender RC, Bayne CJ. Killing of *Schistosoma mansoni* sporocysts by hemocytes from resistant *Biomphalaria glabrata*: role of reactive oxygen species. J Parasitol. 2001 (a); 87(2):292–9. https://doi.org/10.1645/0022-3395(2001)087[0292:KOSMSB]2.0.CO;2 PMID: 11318558

10. Hahn UK, Bender RC, Bayne CJ. Involvement of nitric oxide in killing of *Schistosoma mansoni* sporocysts by hemocytes from resistant *Biomphalaria glabrata*. J Parasitol. 2001 (b); 87(4):778–85. https://doi.org/10.1645/0022-3395(2001)087[0778:IONOIK]2.0.CO;2 PMID: 11534641

11. Bender RC, Broderick EJ, Goodall CP, Bayne CJ. Respiratory burst of *Biomphalaria glabrata* hemocytes: *Schistosoma mansoni*-resistant snails produce more extracellular H2O2 than susceptible snails. J Parasitol. 2005; 91(2):275–9. https://doi.org/10.1645/GE-415R PMID: 15986600

12. Zelck UE, Gege BE, Schmid S. Specific inhibitors of mitogen-activated protein kinase and PI3-K pathways impair immune responses by hemocytes of trematode intermediate host snails. Dev Comp Immunol. 2007; 31(4):321–31. https://doi.org/10.1016/j.dci.2006.06.006 PMID: 16926049

13. Bayne CJ. Successful parasitism of vector snail *Biomphalaria glabrata* by the human blood fluke (trematode) *Schistosoma mansoni*: a 2009 assessment. Mol Biochem Parasitol. 2009; 165(1):8–18. PubMed Central PMCID: PMCPMC2765215. https://doi.org/10.1016/j.molbiopara.2009.01.005 PMID: 19393158

14. Yoshino TP, Coustau C. Immunobiology of *Biomphalaria*-trematode interactions. In: Toledo R, Fried B, editors. *Biomphalaria* snails and larval trematodes. New York: Springer-Verlag; 2011. p. 159–89.

15. Coustau C, Gourbal B, Duval D, Yoshino TP, Adema CM, Mitta G. Advances in gastropod immunity from the study of the interaction between the snail *Biomphalaria glabrata* and its parasites: A review of research progress over the last decade. Fish & shellfish immunology. 2015. Epub 2015/02/11.

16. Wu XJ, Sabat G, Brown JF, Zhang M, Taft A, Peterson N, et al. Proteomic analysis of *Schistosoma mansoni* proteins released during in vitro miracidium-to-sporocyst transformation. Mol biochem parasitol. 2009; 164(1):32–44. Epub 2008/12/20. PubMed Central PMCID: PMC2665799. https://doi.org/10.1016/j.molbiopara.2008.11.005 PMID: 19095013

17. Lodes MJ, Yoshino TP. The effect of schistosome excretory-secretory products on *Biomphalaria glabrata* hemocyte motility. J Invertebr Pathol. 1990; 56(1):75–85. Epub 1990/07/01. PMID: 2376664

18. Connors VA, Yoshino TP. In vitro effect of larval *Schistosoma mansoni* excretory-secretory products on phagocytosis-stimulated superoxide production in hemocytes from *Biomphalaria glabrata*. J Parasitol. 1990; 76(6):895–902. Epub 1990/12/01. PMID: 2174969

19. Connors VA, Lodes MJ, Yoshino TP. Identification of a *Schistosoma mansoni* sporocyst excretory-secretory antioxidant molecule and its effect on superoxide production by *Biomphalaria glabrata* hemocytes. J Invertebr Pathol. 1991; 58(3):387–95. Epub 1991/11/01. PMID: 1664845

20. Vermeire JJ, Yoshino TP. Antioxidant gene expression and function in in vitro-developing *Schistosoma mansoni* mother sporocysts: possible role in self-protection. Parasitol. 2007; 134(Pt 10):1369–78. Epub 2007/04/21.

21. Zahoor Z, Davies AJ, Kirk RS, Rollinson D, Walker AJ. Nitric oxide production by *Biomphalaria glabrata* haemocytes: effects of *Schistosoma mansoni* ESPs and regulation through the extracellular signal-regulated kinase pathway. Parasit Vectors 2009; 2(1):18. https://doi.org/10.1186/1756-3305-2-18 PMID: 19386102

22. Humphries JE, Yoshino TP. *Schistosoma mansoni* excretory-secretory products stimulate a p38 signalling pathway in *Biomphalaria glabrata* embryonic cells. Int J Parasitol 2006; 36(1):37–46. https://doi.org/10.1016/j.ijpara.2005.08.009 PMID: 16194541

23. Zahoor Z, Davies AJ, Kirk RS, Rollinson D, Walker AJ. Larval excretory-secretory products from the parasite *Schistosoma mansoni* modulate HSP70 protein expression in defence cells of its snail host, *Biomphalaria glabrata*. Cell Stress Chaperones 2010; 15(5):639–50. https://doi.org/10.1007/s12192-010-0176-z PMID: 20182834

24. Zahoor Z, Lockyer AE, DA J., Kirk RS, Emery AM, Rollinson D, et al. Differences in the gene expression profiles of haemocytes from schistosome-susceptible and -resistant *Biomphalaria glabrat*a exposed to *Schistosoma mansoni* excretory-secretory products. PLoS One 2014; 9(3):e93215. https://doi.org/10.1371/journal.pone.0093215 PMID: 24663063

25. Hansen EL. A cell line from embryos of *Biomphalaria glabrata* (Pulmonata): Establishment and characteristics In: Maramorosch K, editor. Invertebrate Tissue Culture: Research Applications. New York, NY: Academic Press, Inc. 1976. p. 75–97.

26. Yoshino TP, Coustau C, Modat S, Castillo MG. The *Biomphalaria glabrata* embryonic (BGE) molluscan cell line: Establishment of an in vitro cellular model for the study of snail host-parasite interactions. Malacologia. 1999; 41:331–43.

27. Coustau C, Yoshino TP. Flukes without snails: advances in the in vitro cultivation of intramolluscan stages of trematodes. Exp Parasitol 2000; 94(1):62–6. https://doi.org/10.1006/expr.1999.4462 PMID: 10631085

28. Yoshino TP, Laursen JR. Production of *Schistosoma mansoni* daughter sporocysts from mother sporocysts maintained in synxenic culture with *Biomphalaria glabrata* embryonic (Bge) cells. J Parasitol. 1995; 81(5):714–22. PMID: 7472861

29. Yoshino TP, Bickham U, Bayne CJ. Molluscan cells in culture: primary cell cultures and cell lines. Can J Zool. 2013; 91(6). Epub 2013/11/08. PubMed Central PMCID: PMC3816639. https://doi.org/10.1139/cjz-2012-0258 PMID: 24198436

30. Ivanchenko MG, Lerner JP, McCormick RS, Toumadje A, Allen B, Fischer K, et al. Continuous in vitro propagation and differentiation of cultures of the intramolluscan stages of the human parasite *Schistosoma mansoni*. Proc Natl Acad Sci U S A. 1999; 96(9):4965–70. Epub 1999/04/29. PubMed Central PMCID: PMC21800. PMID: 10220402

31. Feske S, Wulff H, Skolnik EY. Ion channels in innate and adaptive immunity. Annu Rev Immunol 2015; 33:291–353. https://doi.org/10.1146/annurev-immunol-032414-112212 PMID: 25861976

32. Chernin E. Observations on hearts explanted in vitro from the snail Australorbis glabratus. J Parasitol. 1963; 49:353–64. PMID: 14020610

33. Hahn UK, Bender RC, Bayne CJ. Production of reactive oxygen species by hemocytes of *Biomphalaria glabrata*: carbohydrate-specific stimulation. Devel comp immunology. 2000; 24(6–7):531–41. Epub 2000/06/01.

34. Sminia T, Barendsen LA. A comparative morphological an enzyme histochemical study on blood cells of the freshwater snails *Lymnaea stagnalis*, *Biomphalaria glabrata* and *Bulinus truncatus*. J Morphol. 1980; 165:31–9.

35. Capasso M. Regulation of immune responses by proton channels. Immunology. 2014; 143(2):131–7. PubMed Central PMCID: PMCPMC4172129. https://doi.org/10.1111/imm.12326 PMID: 24890927

36. DeCoursey TE, Morgan D, Musset B, Cherny VV. Insights into the structure and function of HV1 from a meta-analysis of mutation studies. J Gen Physiol. 2016; 148(2):97–118. https://doi.org/10.1085/jgp.201611619 PMID: 27481712

37. DeCoursey TE. Voltage-gated proton channels: molecular biology, physiology, and pathophysiology of the H(V) family. Physiol Rev. 2013;(93):599–652.

38. Mahaut-Smith MP. The effect of zinc on calcium and hydrogen ion currents in intact snail neurones. J Exp Biol. 1989; 145:455–64. PMID: 22912993

39. DeCoursey TE, Morgan D, Cherny VV. The voltage dependence of NADPH oxidase reveals why phagocytes need proton channels. Nature. 2003; 422(6931):531–4. https://doi.org/10.1038/nature01523 PMID: 12673252

40. Woodward OM, Willows AO. Dopamine modulation of Ca^{2+} dependent Cl^- current regulates ciliary beat frequency controlling locomotion in *Tritonia diomedea*. J Exp Biol. 2006; 209(Pt 14):2749–64. https://doi.org/10.1242/jeb.02312 PMID: 16809466

41. Pichon YL, Prime L, Benquet P, Tiaho F. Some aspects of the physiological role of ion channels in the nervous system. Eur Biophys J 2004; 33(3):211–26. Epub 2004 Jan 14. https://doi.org/10.1007/s00249-003-0373-0 PMID: 14722689

42. Kodirov SA. The neuronal control of cardiac functions in molluscs. Physiol A Mol Integr Physiol. 2011; 160(2):102–16.

43. Koch HP, Kurokawa T, Okochi Y, Sasaki M, Okamura Y, Larsson HP. Multimeric nature of voltage-gated proton channels. Proc Natl Acad Sci U S A. 2008; 105(25):9111–6. Epub 2008 Jun 26.

44. DeCoursey TE. The Voltage-Gated Proton Channel: A Riddle, Wrapped in a Mystery, inside an Enigma. Biochemistry. 2015; 54(21):3250–68. https://doi.org/10.1021/acs.biochem.5b00353 PMID: 25964989

45. Baeza Garcia A, Pierce RJ, Gourbal B, Werkmeister E, Colinet D, Reichhart JM, et al. Involvement of the cytokine MIF in the snail host immune response to the parasite *Schistosoma mansoni*. PLoS Pathog. 2010; 6(9):e1001115. PubMed Central PMCID: PMCPMC2944803. https://doi.org/10.1371/journal.ppat.1001115 PMID: 20886098

46. Knight M, Ittiprasert W, Odoemelam EC, Adema CM, Miller A, Raghavan N, et al. Non-random organization of the *Biomphalaria glabrata* genome in interphase Bge cells and the spatial repositioning of activated genes in cells co-cultured with *Schistosoma mansoni*. Int J Parasitol. 2011; 41(1):61–70. PubMed Central PMCID: PMCPMC3081665. https://doi.org/10.1016/j.ijpara.2010.07.015 PMID: 20849859

47. Rinaldi G, Yan H, Nacif-Pimenta R, Matchimakul P, Bridger J, Mann VH, et al. Cytometric analysis, genetic manipulation and antibiotic selection of the snail embryonic cell line Bge from *Biomphalaria glabrata*, the intermediate host of *Schistosoma mansoni*. Int J Parasitol. 2015; 45(8):527–35. PubMed Central PMCID: PMCPMC4562316. https://doi.org/10.1016/j.ijpara.2015.02.012 PMID: 25907768

48. Roger E, Gourbal B, Grunau C, Pierce RJ, Galinier R, Mitta G. Expression analysis of highly polymorphic mucin proteins (Sm PoMuc) from the parasite *Schistosoma mansoni*. Mol Biochem Parasitol. 2008; 157(2):217–27. https://doi.org/10.1016/j.molbiopara.2007.11.015 PMID: 18187213

49. Roger E, Mitta G, Mone Y, Bouchut A, Rognon A, Grunau C, et al. Molecular determinants of compatibility polymorphism in the *Biomphalaria glabrata/Schistosoma mansoni* model: new candidates identified by a global comparative proteomics approach. Mol Biochem Parasitol. 2008; 157(2):205–16. https://doi.org/10.1016/j.molbiopara.2007.11.003 PMID: 18083248

50. Mone Y, Gourbal B, Duval D, Du Pasquier L, Kieffer-Jaquinod S, Mitta G. A large repertoire of parasite epitopes matched by a large repertoire of host immune receptors in an invertebrate host/parasite model. PLoS Negl Trop Dis. 2010; 4(9). PubMed Central PMCID: PMCPMC2935394.

51. Mone Y, Ribou AC, Cosseau C, Duval D, Theron A, Mitta G, et al. An example of molecular co-evolution: reactive oxygen species (ROS) and ROS scavenger levels in *Schistosoma mansoni/Biomphalaria glabrata* interactions. Int J Parasitol. 2011; 41(7):721–30. https://doi.org/10.1016/j.ijpara.2011.01.007 PMID: 21329695

52. Humphries JE, Yoshino TP. Regulation of hydrogen peroxide release in circulating hemocytes of the planorbid snail *Biomphalaria glabrata*. Devel comp immunology. 2008; 32(5):554–62. Epub 2007/11/06. PubMed Central PMCID: PMC2271030.

53. Adema CM, Hertel LA, Miller RD, Loker ES. A family of fibrinogen-related proteins that precipitates parasite-derived molecules is produced by an invertebrate after infection. Proc Natl Acad Sci U S A. 1997; 94(16):8691–6. PubMed Central PMCID: PMCPMC23082. PMID: 9238039

54. Pila EA, Tarrabain M, Kabore AL, Hanington PC. A Novel Toll-Like Receptor (TLR) Influences Compatibility between the Gastropod *Biomphalaria glabrata*, and the Digenean Trematode *Schistosoma mansoni*. PLoS Pathog. 2016; 12(3):e1005513. PubMed Central PMCID: PMCPMC4807771. https://doi.org/10.1371/journal.ppat.1005513 PMID: 27015424

55. Zhang SM, Zeng Y, Loker ES. Characterization of immune genes from the schistosome host snail *Biomphalaria glabrata* that encode peptidoglycan recognition proteins and gram-negative bacteria binding protein. Immunogenetics. 2007; 59(11):883–98. PubMed Central PMCID: PMCPMC3632339. https://doi.org/10.1007/s00251-007-0245-3 PMID: 17805526